

## International Journal of Pharmacology

ISSN 1811-7775





ISSN 1811-7775 DOI: 10.3923/ijp.2025.453.463



### **Research Article**

### Effects of Loading TAB2 siRNA and Cisplatin Nano-Liposomes Mediated Macrophage Polarization on Drug Resistance, Proliferation and Metastasis of Ovarian Cancer Cells

Bo Li and Shuping Li

Department of Obstetrics and Gynecology, The Fourth Hospital of Changsha, Changsha, 410006, Hunan, China

### **Abstract**

Background and Objective: Tumor cell reduction surgery combined with cisplatin chemotherapy can achieve remission in ovarian cancer (OC) patients, but most patients will experience recurrence. This work investigated the effects of co-loading Small Interfering RNA (siRNA) targeting transforming growth factor-beta activated kinase 1 binding protein 2 (TAB2) and cisplatin in nano-liposomes, mediated by macrophage M2 polarization, on drug-resistant OC cell proliferation and migration. Materials and Methods: Bone Marrow-Derived Macrophage (BMDM) was obtained from mouse bone marrow and interleukin-5 induced M2 polarization of the cells. A cisplatinresistant OC cell model (ID8/R) was prepared using the cisplatin gradient exposure method. Normal culture was used as the Ctrl group and co-loaded negative control, TAB2 siRNA and cisplatin-loaded nanoliposomes (siNC-DDP-LNP and siTAB2-dDP-LNP) were transfected to detect the activation status of M2 type BMDM. The BMDM-conditioned medium was added and cell proliferation and migration were detected. Results: The prepared siNC-DDP-LNP and siTAB2-DDP-LNP possessed similar circular morphology with a PS of around 100 nm. The siRNA EE was >90% and the drug LC was  $>0.14 \mu g/\mu L$ . After transfection, the siTAB2-DDP-LNP group showed a great reduction in TAB2 (p<0.05). Following BMDM identification, the M1 type markers (iNOS and TNF- $\alpha$  expression, average fluorescence intensity (FI) of CD80 and CD86) decreased, while the M2 type markers (Arg1 and MgI1 expression, average FI of CD206 and CD163) increased, with sharp differences (p<0.05). After transfection with BMDM conditioned medium and nano-liposomes, the siTAB2-DDP-LNP group presented greatly increased average FI values of CD80, CD86 and CD40, decreased cell viability and reduced count of migrated cells, exhibiting great differences after comparison (p < 0.05). **Conclusion:** The siTAB2/DDP-LNP effectively activated tumor-associated macrophage polarization, thereby achieving effective killing of drug-resistant OC cells (OCCs).

Key words: Nano-liposomes, transforming growth factor-beta activated kinase 1 (TAK1) binding protein 2, small interfering RNA, drug-resistant OCCs, macrophage polarization

Citation: Li, B. and S. Li, 2025. Effects of loading TAB2 siRNA and cisplatin nano-liposomes mediated macrophage polarization on drug resistance, proliferation and metastasis of ovarian cancer cells. Int. J. Pharmacol., 21: 453-463.

Corresponding Author: Bo Li, Department of Obstetrics and Gynecology, The Fourth Hospital of Changsha, Changsha, 410006, Hunan, China

Copyright: © 2025 Bo Li and Shuping Li. This is an open access article distributed under the terms of the creative commons attribution License, which permits unrestricted use, distribution and reproduction in any medium, provided the original author and source are credited.

Funding: This work was supported by Scientific Research Project of Hunan Provincial Health Commission in 2023 (No. D202305016815).

Competing Interest: The authors have declared that no competing interest exists.

Data Availability: All relevant data are within the paper and its supporting information files.

### **INTRODUCTION**

Ovarian cancer (OC) is a gynecologic malignancy with insidious onset, rapid progression and a lack of specific diagnostic methods. Most patients are diagnosed with extensive intraperitoneal metastasis, leading to a high mortality rate<sup>1</sup>. Radiotherapy is a primary non-surgical treatment for malignant tumors and cisplatin, an effective and broad-spectrum anticancer drug, has been widely used in treating various diseases, especially in different cancers<sup>2,3</sup>. Tumor ablation combined with cisplatin is a common therapeutic approach for OC, with 80% of patients being sensitive to this chemotherapy regimen. However, the recurrence rate is over 60%<sup>4,5</sup>. Cisplatin not only kills cancer cells but also causes damage to normal cells and severe toxicity, making it unsuitable for long-term treatment.

Gene therapy is a novel treatment technique that involves introducing exogenous gene fragments into cancer cells to regulate aberrant genes, enhance the host's anti-tumor immunity and increase the tumor's sensitivity to radiotherapy/chemotherapy<sup>6</sup>. Gene therapy carriers can be classified as viral vectors and non-viral vectors. Cationic liposomes offer advantages such as natural fusion, nonimmunogenicity and repeatable transfection, making them highly sought after<sup>7</sup>. Furthermore, liposomes are mature carriers and economical and effective anti-cancer liposomal drugs have been successfully developed. By embedding drugs within liposomes, matrix adsorption, entrapment and adhesion effects can reduce drug dissolution, diffusion rate, distribution coefficient, etc., prolong drug release time, reduce toxicity and enhance stability<sup>8</sup>. Research on cisplatin liposomal formulations is abundant, as they can enhance the anti-tumor effects of cisplatin and reduce toxic reactions9. With the rapid development of nanotechnology, nano-liposomes offer new approaches for local drug absorption, constructing drug release systems and improving drug delivery methods. Nanoliposomes consist of ionizable lipids, cholesterol and polyethylene glycol substances, which enable them to escape phagocytosis by macrophages in the body and achieve passive targeting<sup>10</sup>. The use of nano-liposomes to construct drug delivery systems has several advantages 11,12. Firstly, it has excellent biocompatibility due to the carrier being composed of phospholipid bilayer-enclosed aqueous vesicles. Secondly, it exhibits broad adaptability to loaded drugs, accommodating water-soluble drugs in the aqueous phase, lipid-soluble drugs in the lipid membrane and amphiphilic drugs on the lipid membrane, allowing simultaneous loading of hydrophilic and hydrophobic drugs. Thirdly, high bioavailability as phospholipids are the main components of cell membranes,

rendering them non-toxic upon entry into the body and unlikely to trigger an immune response. Fourthly, it shows good protection of loaded drugs, preventing dilution by body fluids and degradation by endogenous enzymes. Evers *et al.*<sup>13</sup> have shown that nano-liposomes achieve nearly 100% loading efficiency for nucleic substances. The nano-carriers hold promise for the co-delivery of Small Interfering RNA (siRNA) and chemotherapeutic agents, thereby enabling comprehensive treatment of drug-resistant tumors.

In this work, nano-liposomes co-loaded with TAB2 siRNA and cisplatin drugs were prepared and their effects on the proliferation and migration of drug-resistant OC cells (OCCs) were investigated in the presence of macrophage M2 polarization. It aimed to investigate the roles of TAB2 gene silencing on cisplatin resistance in OC and to explore new therapeutic approaches for treating cisplatin-resistant OC.

### **MATERIALS AND METHODS**

**Study area:** The study was conducted at The Fourth Hospital of Changsha from January, 2023 to December, 2023.

Preparation of co-loaded TAB2 siRNA and cisplatin nano-

# **liposomes:** Following a 2:1 molar ratio, cationic lipids (2,3-dioleyloxypropyl) trimethylammonium chloride (DOTAP, Xi'an Qiyue Biotechnology Co., Ltd., China) and cholesterol were taken and dissolved in chloroform solution. Subsequently, the solution was subjected to rotary evaporation for 1 hr to form a lipid film. Next, 1 mL of 1 mg/mL cisplatin deionized water solution (MedChemExpress, China) was added and the lipid

a lipid film. Next, 1 mL of 1 mg/mL cisplatin deionized water solution (MedChemExpress, China) was added and the lipid film was dispersed using water bath ultrasound and thin-film extrusion methods. Then, TAB2 siRNA solution was mixed to prepare nano-liposomes co-loaded with cisplatin and TAB2 siRNA, named siTAB2-DDP-LNP. Using the same method, nano-liposomes co-loaded with negative control siRNA and cisplatin were prepared, which was named siNC-DDP-LNP.

**Characterization of co-loaded TAB2 siRNA and cisplatin nano-liposomes:** The nano-liposomes PS and SZP were analyzed using a Nicomp Z3000 nanoparticle size and zeta potential analyzer (PSSPSS, USA). Additionally, the morphology of the nano-liposomes was observed under an HT7800 transmission electron microscope (Hitachi, Japan).

The EE of siRNA was determined using Multiskan SkyHigh UV-Vis spectrophotometer (Hash, USA) and the encapsulation efficiency of siRNA was calculated. Each nano-liposome particle was lysed in a methanol-water solution with a molar ratio of 55:45.

High-Performance Liquid Chromatography (HPLC) was employed to further detect the cisplatin DL. Each nanoliposome particle (1 g) was implemented with a dissolution in 15 mL anhydrous ethanol and after ultrasonic emulsification and uniform dispersion, with a final volume of 50 mL. The mixture was then subjected to a 10 min centrifugation at 12,000 rpm for supernatant collection to prepare solution A after filtration through a 0.45 µm microporous membrane. Another 1 g sample was dissolved in ultrapure water and solution B was prepared following the same method. The content of cisplatin in solution A and B were measured and the DL was calculated.

Cell treatments: Mouse ovarian cancer ID8 cells (Aoruisai Biological Cell Bank, China) were inoculated in RPMI-1640 culture medium (Gibco, USA) with 10% fetal bovine serum (Gibco, USA) and 1% Penicillin Streptomycin (Gibco, USA), 37°C, 5% CO<sub>2</sub> and 100% humidity. Cisplatin-resistant OCCs (ID8/R) were selected using the cisplatin gradient exposure method of Oh et al.14 and were cultured in a low-concentration cisplatin solution (0.5 µmol/L) for 48 hrs and then moved to cisplatin-free medium for 48 hrs of recovery. This process was repeated three times, gradually increasing the cisplatin concentration in the culture by 0.5 µmol/L each time, until reaching a final cisplatin concentration of 4.0 µmol/L. The ID8/R cells were seeded and then transfected with siNC-DDP-LNP and siTAB2-DDP-LNP at a final siRNA concentration of 150 nmol/L, followed by a 72 hrs incubation period.

Detection of cell TAB2 interference efficiency: The ID8/R cells were seeded and treated differently, followed by 48 hrs of continuous incubation. Extraction of total RNA from the cells was implemented using the Trizol method of Zhang et al.<sup>15</sup> and utilizing the first strand cDNA synthesis kit (Beijing Baori (Takara Bio) Biotechnology Co., Ltd., China), reverse transcribed into cDNA. Expression changes of the TAB2 gene were then detected using a Fluorescent Quantitative PCR Reagent kit (Beijing Baori (Takara Bio) Biotechnology Co. Ltd., China). The primer information for qPCR was as follows: Upstream and downstream primers for TAB2: 5'-ATTTCTG GTCTACGCAATCACAT-3' and 5'-ACTAACGCT GTGTGTTAAAGTCC-3' and those for GAPDH: 5'-AGGTCGGT GTGAACGGATTTG-3' and 5'-TGTAGACCATGTAGTTGAGGT-3'. The GAPDH was used as the internal reference gene and the level of the TAB2 gene was determined using the  $2^{-\Delta aCt}$ method<sup>16</sup>. The above steps were taken thrice for better accuracy.

**Extraction of BMDM and M2 type induction:** Five adult male Balb/C mice (Beijing Biou Biotechnology Co., Ltd., China) were intraperitoneally injected with 20 mg/kg of 1% pentobarbital sodium for anesthesia and euthanized by cervical dislocation. Under sterile conditions, bone marrow was taken from the thigh bone and BMCs were flushed out by injecting phosphate-buffered saline into the marrow cavity. The cells were then treated with red blood cell lysis buffer. The BMDM cells were obtained by culturing the cells in a complete medium containing 20 ng/mL macrophage colony-stimulating factor (MCSF, Sigma-Aldrich, USA) for 5 days. The M2-type BMDMs were obtained by inducing BMDM cells with 20 ng/mL interleukin-5 (Sigma Aldrich, USA) for 24 hrs. The fqPCR was applied to examine M1-type macrophage-related genes iNOS and TNF- $\alpha$  and M2-type macrophage-related genes Arg1 and Mgl1. The primer sequences for fgPCR were as follows: Upstream and downstream primers of iNOS: 5'-GGAGTGACG GCAAACATGACT-3' and 5'-TCGATGCACAACTGGGTGAAC-3'; those of TNF-α: 5'-GACGTGGAACTGGCAGAAGAG-3' and 5'-TTGGTGGTTTGTGAGTGTGAG-3'; those of Arg1: 5'-CTCCA AGCCAAAGTCCTTAGAG-3' and 5'-AGGAGCTGTCATTAGGGA CATC-3'; and those of Mgl1:5'-CTGCTCGTAGCTGGCAATACA-3' and 5'-CCGGTAATCATCTGGCACACT-3'. The CD80, CD86, CD206 and CD163 were measured using CytoFLEX flow cytometer (Beckman Kurt Company, USA). The experiment was repeated three times for accuracy.

FCT to judge activation of M2-type BMDM cells: The ID8/R cells were seeded in Transwell chambers at  $1 \times 10^5$  cells. Following the drug administration method described in section 2.4, the ID8/R cells treated with siNC-DDP-LNP and siTAB2-DDP-LNP for 24 hrs were used as the control group (Ctrl). For the experimental (Exp) group, they were transferred to the lower part of the Transwell and co-cultured with M2-type BMDM cells at  $1 \times 10^5$  cells. After 24 hrs of co-culture, BMDM cells were sealed in PBS with 2% bovine serum albumin for 30 min. Fluorescent-labeled anti-mouse CD80, CD86 or CD40 antibodies were added and BMDM cells were incubated under dark conditions for 30 min. After centrifugation, the cells were resuspended in PBS and average fluorescence intensity (FI) was determined using an CytoFLEX flow cytometer. To ensure accuracy, the above operations were allowed to be taken three times.

**CCK-8 to detect ID8/R cells survival:** After collecting the activated BMDM conditioned medium, ID8/R cells were seeded at  $8 \times 10^3$  cells. Then, a mixture of BMDM conditioned

medium and RPMI-1640 containing siNC-DDP-LNP and siTAB2-DDP-LNP in a 1:1 ratio was added for co-culture and the ID8/R cells were incubated together for 24 hrs. Cells cultured solely in a complete medium served as the control group (Ctrl). The cell viability of each well was examined using a CCK-8 kit (MedChemExpress, China). Again, three experiments were required.

Transwell to assess ID8/R cell migration: The ID8/R cells at  $2 \times 10^5$  cells/mL contained in serum-free culture medium were added to the upper chamber of the Transwell. In the lower chamber, 500 µL of BMDM-conditioned medium was added and the cells were co-cultured for 24 hrs. After removing the liquid from the upper chamber, the cells were immersed in phosphate buffer (Thermo Fisher, USA) for 5 min and then fixed with 4% paraformal dehyde for 20 min. The Transwell was then taken out and a 5 g/L crystal violet solution was added for staining for 25 min. After staining, the Transwell was washed three times with PBS and left to dry inverted. Using a clean cotton swab, any non-migrated cells in the upper chamber were wiped away. Five random fields of view (FOV) were selected under a KP-ICX41M-63M microscope (Shenzhen Koppace Technology Co., Ltd., China) for cell counting and the experiment was repeated thrice, too.

**Statistical analysis:** The data were processed using SPSS 22.0 and all values were expressed as Mean±Standard Deviation. One-way analysis of variance was utilized to compare multiple groups and pairwise comparisons were performed using t-tests. As p<0.05 was considered statistically significant.

### **RESULTS**

### Characterization of co-loaded siRNA and cisplatin nano-

**liposomes:** In this study, nano-liposomes co-loaded with siRNA and cisplatin were prepared and characterized. As displayed in Fig. 1, the prepared siNC-DDP-LNP and siTAB2-DDP-LNP nano-liposomes exhibited a spherical morphology with average diameters of (103.9 $\pm$ 5.8) nm and (96.4 $\pm$ 6.7) nm, respectively. Their SZPs were (26.6 $\pm$ 4.4) mV and (32.3 $\pm$ 3.7) mV, respectively. The siRNA ER values were (91.9 $\pm$ 5.2%) and (92.7 $\pm$ 5.8%), respectively, while the cisplatin LCs were (0.15 $\pm$ 0.03) and (0.14 $\pm$ 0.04) µg/µL, respectively. Figure 1a shows the electron microscopy image of liposomes, Fig. 1b shows the average diameter of liposomes, Fig. 1c shows the surface Zeta potential of liposomes, Fig. 1d shows the encapsulation efficiency of liposome siRNA and Fig. 1e shows the cisplatin loading capacity of liposomes.

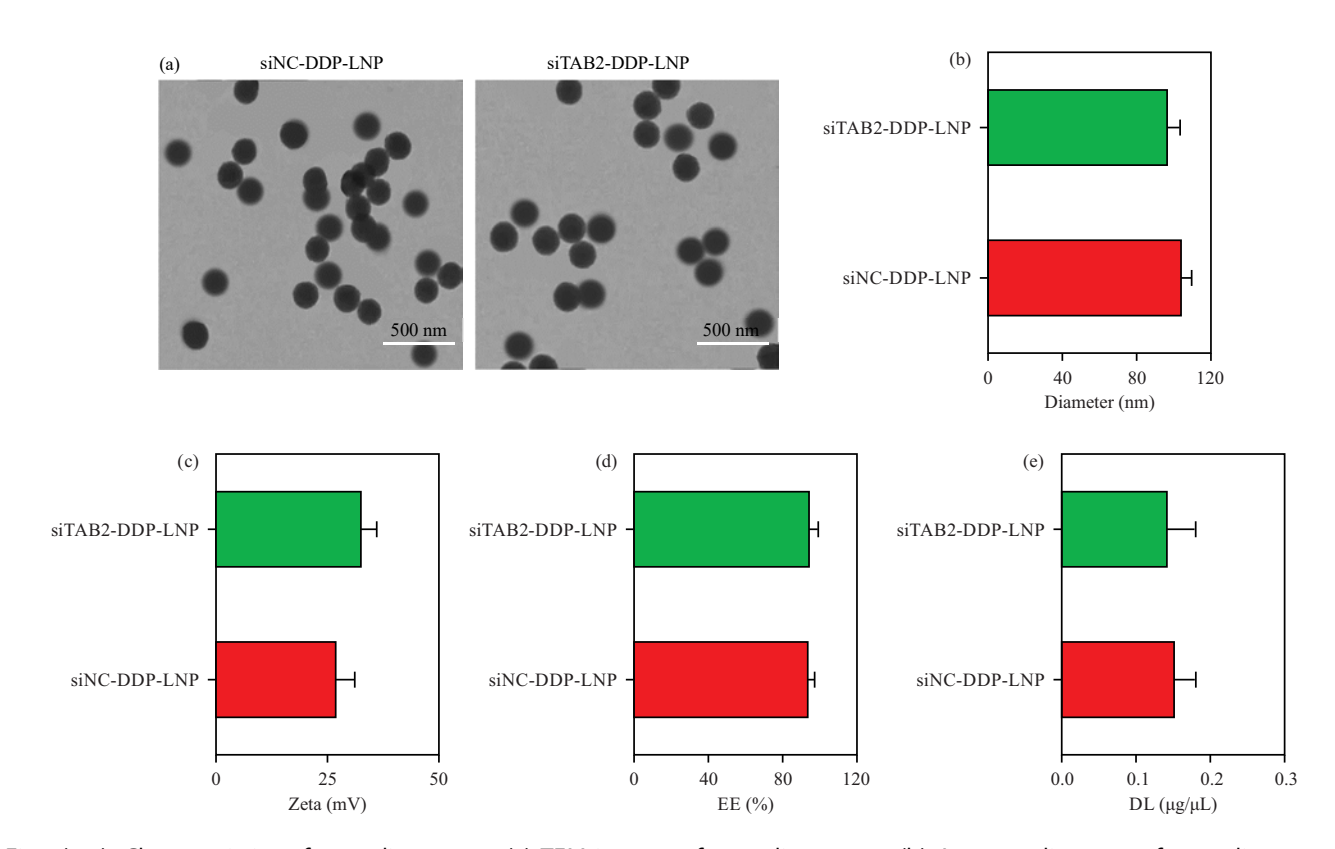


Fig. 1(a-e): Characteristics of nano-liposomes, (a) TEM images of nano-liposomes, (b) Average diameter of nano-liposomes, (c) SZP of nano-liposomes, (d) siRNA EE and (e) Cisplatin LC

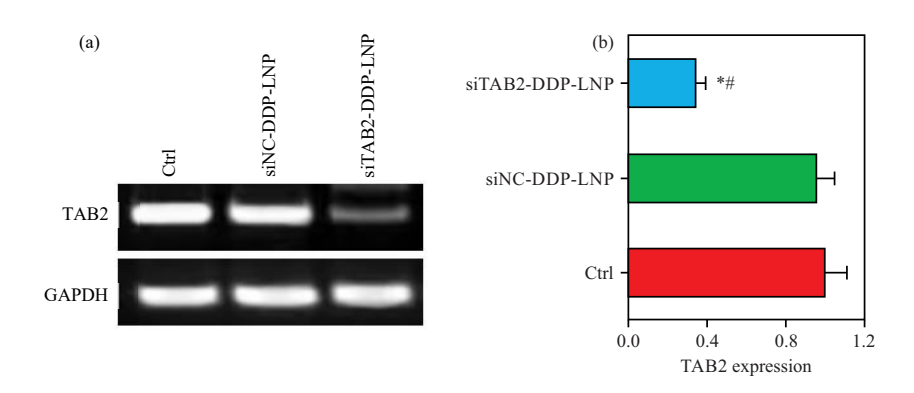


Fig. 2(a-b): Detection results of TAB2 mRNA, (a) PCR results and (b) Level of TAB2 mRNA \*Compared with Ctrl group, p<0.01 and \*Compared with siNC-DDP-LNP group, p<0.05

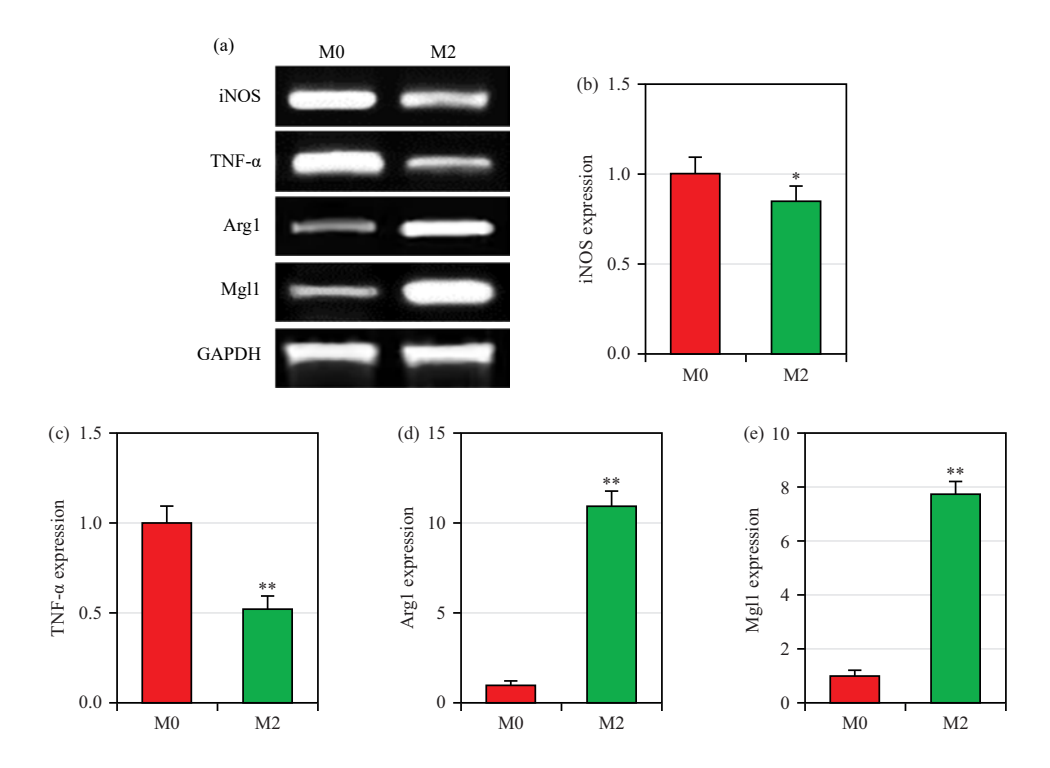


Fig. 3(a-e): Expressions of mRNA in M0 and M2 type relevant proteins, (a) PCR results and (b-e) mRNA contents in iNOS, TNF- $\alpha$ , Arg1 and Mgl1, respectively

\*Compared with M0 type, p<0.05 and \*\*Compared with M0 type, p<0.01

**TAB2 level after transfecting siRNA and cisplatin nanoliposomes:** In this work, fqPCR detected the mRNA of TAB2 in cells transfected with siNC-DDP-LNP and siTAB2-DDP-LNP to assess the silencing efficiency. Figure 2a shows the PCR product detection of TAB2 expression and Fig. 2b shows the statistical results of relative expression of TAB2), no visible difference in TAB2 was observed between the siNC-DDP-LNP and Ctrl groups (p>0.05). However, the siTAB2-DDP-LNP group exhibited sharply lower TAB2 in

contrast to the Ctrl group and the siNC-DDP-LNP group (p<0.05).

**Identification of M2-type BMDM:** In this work, polarization of mouse BMDMs were introduced using MCSF and IL5 for identification. As demonstrated in Fig. 3a, the detection of PCR products of each target gene expression and Fig. 3(b-e) show the relative expression results of iNOS, TNF- $\alpha$ , Arg1 and Mgl1, respectively and Fig. 4(a-d) show the

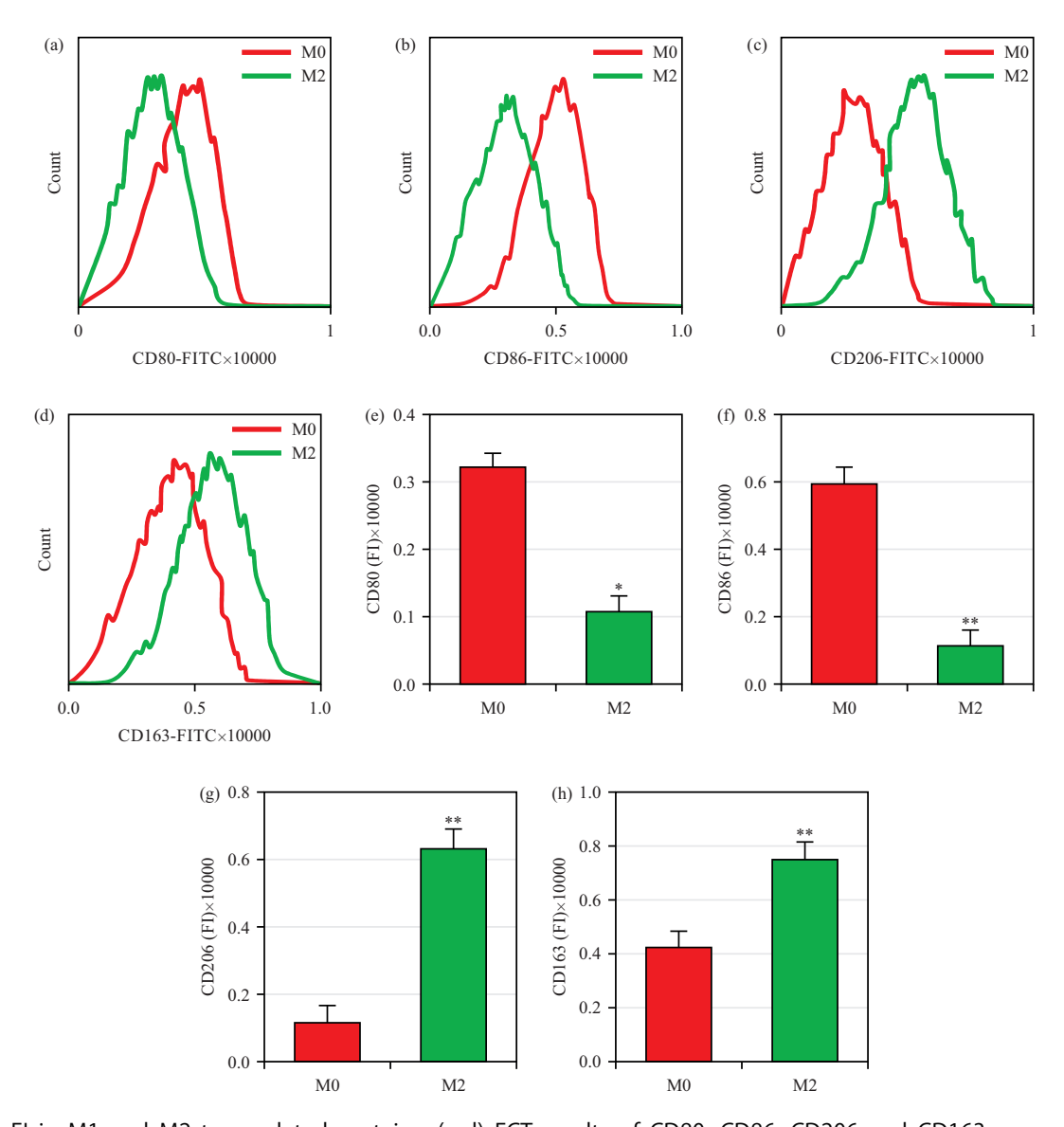


Fig. 4(a-h): FI in M1 and M2 type related proteins, (a-d) FCT results of CD80, CD86, CD206 and CD163, respectively and (e-h) Average FI levels of CD80, CD86, CD206 and CD163, respectively

\*\*Compared with M0 type and p<0.01

fluorescence detection flow cytometry of M0 and M2 macrophage associated proteins, respectively. Figure 4(e-h) show the average fluorescence intensity of M0 and M2 macrophage-associated proteins, respectively, mRNA levels in M2 markers, iNOS and TNF- $\alpha$ , were considerably reduced after induction, while those in Arg1 and Mg11 were increased sharply. The average FI values of CD80 and CD86 were reduced, whereas those of CD206 and CD163 were observably increased, showing great differences (p<0.05).

**Effects of co-loaded siRNA and cisplatin nano-liposomes on drug-resistant M2-type BMDM cells:** In this work, FCT detected changes in the state of cisplatin drug-resistant OCCs

M2-type macrophages after transfection with siNC-DDP-LNP and siTAB2-DDP-LNP. Figure 5(a-f) show the average fluorescence intensity changes of M0 and M2 macrophage-associated proteins, respectively, the average FI values of CD80, CD86 and CD40 in cells transfected with siNC-DDP-LNP and siTAB2-DDP-LNP were much lower to those in the Ctrl group and siNC-DDP-LNP group, showing obvious differences (p<0.05).

Effects of co-loaded siRNA and cisplatin nano-liposomes mediated BMDM reverse polarization on proliferation and migration of drug-resistant OCCs: In this study, the effects of siNC-DDP-LNP and siTAB2-DDP-LNP-mediated M2

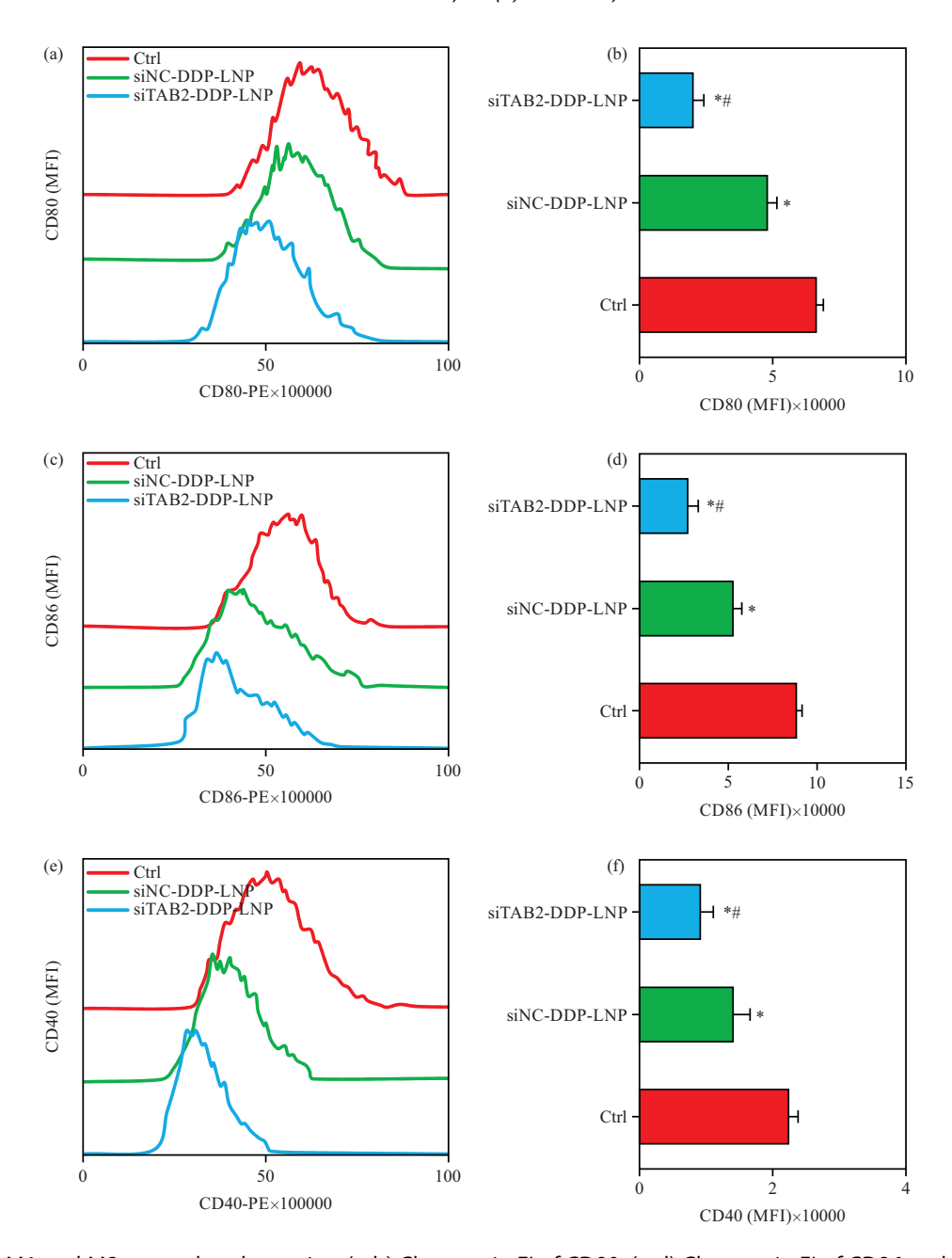


Fig. 5(a-f): FI in M1 and M2 type related proteins, (a-b) Changes in FI of CD80, (c-d) Changes in FI of CD86 and (e-f) Changes in FI of CD40

\*Compared with Ctrl group, p<0.01 and \*Compared with siNC-DDP-LNP group, p<0.05

macrophage polarization on the proliferation and migration of cisplatin drug-resistant OCCs were analyzed using CCK-8 and Transwell assays. As demonstrated in Fig. 6 and 7 (Fig. 7a shows the observation of cell migration staining, while Fig. 7b shows the comparison of the number of migrating cells in each group), counts of proliferated and migrated cells were greatly less in cells transfected with siNC-DDP-LNP and siTAB2-DDP-LNP based on those in the Ctrl group (p<0.05). Furthermore, those were also less in cells transfected with

siTAB2-DDP-LNP in comparison to those after transfection by siNC-DDP-LNP group (p<0.05).

### **DISCUSSION**

In reproductive organ tumors, OC has the second highest incidence after cervical cancer (CC) and endometrial cancer, but it has the highest mortality rate. Approximately 75% of OC cases are diagnosed at an advanced stage, so its 5-year

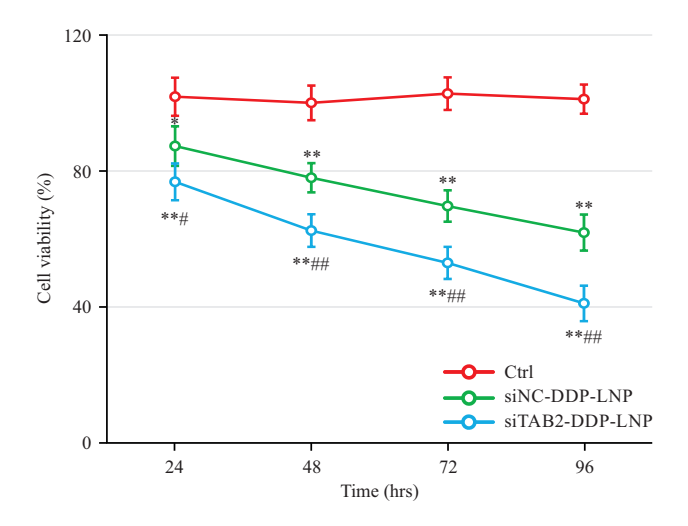


Fig. 6: Proliferation of drug-resistant OCCs

\*Compared with Ctrl group, p<0.05, \*\*Compared with Ctrl group, p<0.01, \*Compared with Ctrl group, p<0.05 and \*\*Compared with siNC-DDP-LNP group, p<0.01

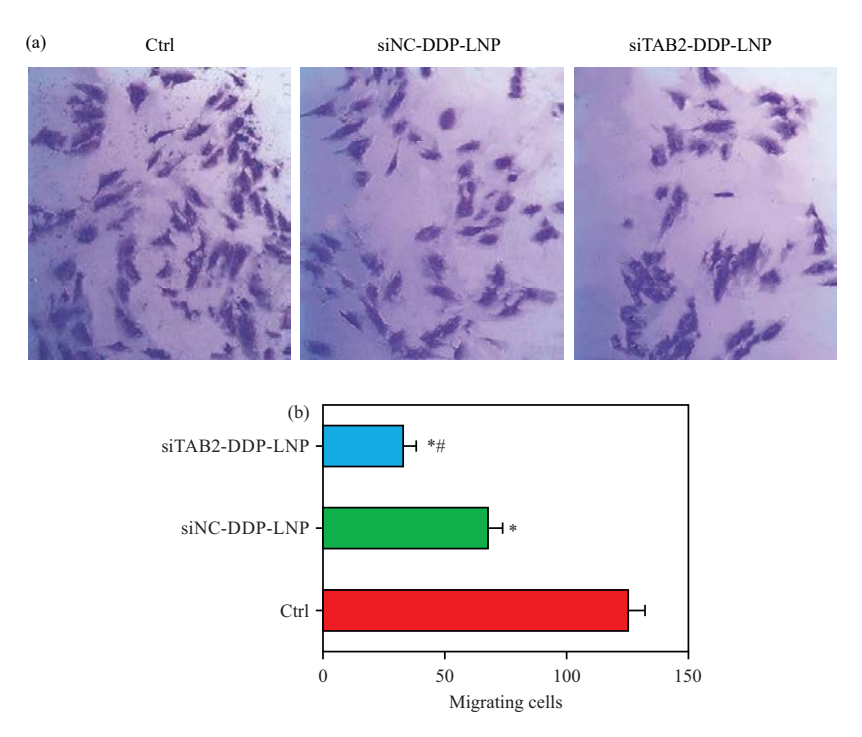


Fig. 7(a-b): Migration of drug-resistant OCCs, (a) Transwell transfection staining results (×200) and (b) Count of migrated cells \*Compared with Ctrl group, p<0.01 and \*Compared with siNC-DDP-LNP group, p<0.05

survival rate is extremely low. Macrophages are important immune and inflammatory cells in the body, characterized by high genomic stability and no resistance issues<sup>17</sup>. The current treatment modalities for tumors include surgery, radiotherapy, chemotherapy and biological therapy. The combination of radiotherapy with radiosensitizers can enhance the effectiveness of radiation in killing tumor cells<sup>18</sup>. Cisplatin, a commonly used antineoplastic drug in clinical practice,

exhibits a radio-sensitizing effect. It can be utilized in the treatment of various tumors due to its cytotoxic properties, which not only kill tumor cells but also inhibit their repair mechanisms, while also acting as a radiosensitizer<sup>19,20</sup>.

However, cisplatin can cause significant harm to normal cells in the body, making prolonged drug treatment infeasible for patients. The preparation of nano-liposomes loaded with anticancer drugs can reduce the drug's toxicity while

increasing its antitumor efficacy. The present study prepared nano-liposomes (siTAB2-DDP-LNP) co-encapsulating TAB2 siRNA and cisplatin. Characterization analysis confirmed the successful construction of nanoparticles carrying TAB2 siRNA and cisplatin, with a TAB2 siRNA encapsulation efficiency of 92.7% and a cisplatin drug loading of 0.14  $\mu$ g/ $\mu$ L. For *in vivo* applications, siRNA requires suitable delivery carriers to prevent degradation and inactivation. Cationic lipid carriers have the advantages of natural degradation and lack of immunogenicity, making them commonly applied in gene therapy for tumors<sup>21</sup>. Above results confirm the successful preparation of cisplatin nano-liposomes co-loaded with siNC and siTAB2 in this work.

The downstream signaling pathway of TLRs includes MyD88, IL-1R -associated protein kinase, TRAF6, TAK1, TAB1 and TAB2<sup>22,23</sup>. It has demonstrated that degradation or deficiency of TAB2 effectively inhibits the activation of TAK1 and related inflammatory responses, as reported in many studies<sup>24,25</sup>. Reineri et al.<sup>26</sup> showed that the knockout of TAB2 can restore the sensitivity of tamoxifen-resistant breast cancer (BC) cells to the drug. Guan et al.27 analyzed the role of the circular RNA-WHSC1/miR-7/TAB2 axis in Non-Small Cell Lung Cancer (NSCLC) and confirmed that circ-WHSC1 acts as a sponge to regulate TAB2 by absorbing miR-7, thereby controlling the NSCLC progression. Consequently, TAB2 participates in various cancers. The present study examined the changes in TAB2 expression levels after transfection of siTAB2-DDP-LNP into cells and found a significant decrease in TAB2 expression levels within the cells. These results demonstrated that the siTAB2-DDP-LNP prepared effectively downregulates the TAB2 gene in cells, laying the foundation for subsequent research.

Tumor recurrence and metastasis are important factors leading to patient mortality. Macrophages are the most abundant in OC metastatic microenvironment and exhibit high plasticity. Depending on individual localization and microenvironmental differences, macrophages are classified into classically activated M1-type macrophages and selectively activated M2-type ones, which can undergo mutual transformation under certain conditions<sup>28,29</sup>. The M1-type macrophages can secrete cytokines to promote antigen presentation, thus exerting an anti-tumor effect by modulating the immune response of the body<sup>30</sup>. In contrast, M2-type macrophages have impaired antigen-presenting ability, leading to tumor growth after inhibition of the body's anti-tumor immune response<sup>31</sup>. Additionally, M2-type macrophages can release angiogenic factors and extracellular matrix modulators, directly or indirectly promoting tissue remodeling, angiogenesis and tumor metastasis<sup>32</sup>. The M2-type macrophages are primarily activated by the inflammatory cytokine IL-4 and secrete IL-10 to suppress M1-type macrophages. They play a crucial role in tissue repair, angiogenesis and wound healing<sup>33</sup>. The M2-type macrophages release cell factors like VEGF and Arg-1 and secrete chemokines like CCL17, which attract Th2 cells, eosinophils and basophils, promoting the generation of various metalloproteinases and facilitating cancer cell metastasis<sup>34,35</sup>. The CD80, CD86 and CD40 are molecules located on the surface of M2-type macrophages and are used for assessing M2 macrophage activation<sup>36</sup>. In this study, mouse BMDMs were polarized using MCSF and IL-5 induction. It was observed that the expression levels of M2 markers iNOS and TNF- $\alpha$  decreased, while the expression levels of Arg1 and Mal1 increased. Additionally, the fluorescence intensity of CD80 and CD86 decreased, while the fluorescence intensity of CD206 and CD163 increased. The M2-type macrophages are characterized by elevated CD206 and CD163 on their surface as well as upshifted IL-10 and Arginase 1, whereas M1-type ones exhibit elevated CD40, CD80 and CD8637 as well as upregulated iNOS, TNF- $\alpha$ , IL-1 $\beta$  and IL-12<sup>38</sup>. Lin *et al.*<sup>39</sup> have shown a close relationship between M2 tumor-associated macrophages and the progression and prognosis of OC. Due to the frequent resistance of OC to platinum-based chemotherapy drugs, macrophages have become an ideal target for OC treatment. Furthermore, this study found that after transfection with siTAB2-DDP-LNP, the fluorescence intensity of CD80, CD86 and CD40 decreased in cisplatinresistant ovarian cancer cells. Additionally, both cell proliferation activity and migration were significantly reduced. This indicates that siTAB2-DDP-LNP can inhibit the M2 polarization of macrophages induced by cisplatin in ovarian cancer-resistant cells and suppress both the proliferation and migration of these cells. Taken together, the results herein confirm the successful induction of M2-type macrophages. Huang et al.40 assessed the correlation between TAB2 gene polymorphisms and epithelial ovarian cancer (EOC) and found that the rs237028 was linked with EOC under the allelic and dominant genetic models. Nevertheless, no visible correlation was visualized between the rs237028 and the overall survival rate. Therefore, it is speculated that TAB2 could be a potential target to enhance the sensitivity of drug-resistant OC to chemotherapy. Previously, Zhou et al.41 found that upregulation of TAB2 is linked to CC stem cell-like characteristics and knocking out TAB2 reduces the number of stem cells in CC cells and promotes disease progression, suggesting that TAB2 can be a therapeutic target for overcoming tumor recurrence and chemotherapy resistance by blocking stem cell maintenance. Combining the results from this work, it can be confirmed that siTAB2-DDP-LNP blocks the M2 polarization of cisplatin-resistant OCCs macrophages, thereby enhancing the sensitivity of cells to cisplatin and exerting a cytotoxic effect on tumor cells.

### **CONCLUSION**

The prepared co-loaded TAB2 siRNA and cisplatin nanoliposomes successfully suppressed TAB2 in the cells. Transfection with siTAB2-DDP-LNP effectively inhibited M2 macrophage polarization and enhanced the sensitivity of cisplatin drug-resistant OCCs to the drug, leading to efficient tumor cell killing. This work solely explored the effects of co-loaded TAB2 siRNA and cisplatin nano-liposomes on macrophage polarization, drug resistance, proliferation and migration of OCCs using an *in vitro* cell model. In the future, animal models should be established to further investigate the mechanisms of action of these nano-liposomes on OC metastasis. In conclusion, the results yielded new research insights to address the issue of cisplatin resistance in OC treatment.

### SIGNIFICANCE STATEMENT

To improve the chemotherapy efficacy of ovarian cancer and address issues such as chemotherapy resistance, nanoliposomes co-loaded with TAB2 siRNA and cisplatin drugs were prepared. They can inhibit cell proliferation and induce apoptosis by regulating the polarization of ID8/R macrophages in ovarian cancer resistant cells. The combined application of siRNA nano-delivery systems and chemotherapy drugs is expected to become a new treatment model for addressing chemotherapy resistance.

### REFERENCES

- Morand, S., M. Devanaboyina, H. Staats, L. Stanbery and J. Nemunaitis, 2021. Ovarian cancer immunotherapy and personalized medicine. Int. J. Mol. Sci., Vol. 22. 10.3390/ijms22126532.
- Fournel, L., Z. Wu, N. Stadler, D. Damotte and F. Lococo et al., 2019. Cisplatin increases PD-L1 expression and optimizes immune check-point blockade in non-small cell lung cancer. Cancer Lett., 464: 5-14.
- Wang, H., S. Guo, S.J. Kim, F. Shao and J.W.K. Ho et al., 2021. Cisplatin prevents breast cancer metastasis through blocking early EMT and retards cancer growth together with paclitaxel. Theranostics, 11: 2442-2459.
- 4. Chambers, L.M., E.L.E. Rhoades, R. Bharti, C. Braley and S. Tewari *et al.*, 2022. Disruption of the gut microbiota confers cisplatin resistance in epithelial ovarian cancer. Cancer Res., 82: 4654-4669.
- 5. Dou, Z., C. Qiu, X. Zhang, S. Yao and C. Zhao *et al.*, 2022. HJURP promotes malignant progression and mediates sensitivity to cisplatin and WEE1-inhibitor in serous ovarian cancer Int. J. Biol. Sci., 18: 1188-1210.

- 6. Leidner, R., N.S. Silva, H. Huang, D. Sprott and C. Zheng *et al.*, 2022. Neoantigen T-cell receptor gene therapy in pancreatic cancer. N. Engl. J. Med., 386: 2112-2119.
- Rayamajhi, S., J. Marchitto, T.D.T. Nguyen, R. Marasini, C. Celia and S. Aryal, 2020. pH-responsive cationic liposome for endosomal escape mediated drug delivery. Colloids Surf. B: Biointerfaces, Vol. 188. 10.1016/j.colsurfb.2020.110804.
- 8. Tenchov, R., R. Bird, A.E. Curtze and Q. Zhou, 2021. Lipid nanoparticles-from liposomes to mRNA vaccine delivery, a landscape of research diversity and advancement. ACS Nano, 15: 16982-17015.
- Zhang, J., Y. Pan, Q. Shi, G. Zhang and L. Jiang et al., 2022. Paclitaxel liposome for injection (Lipusu) plus cisplatin versus gemcitabine plus cisplatin in the first-line treatment of locally advanced or metastatic lung squamous cell carcinoma: A multicenter, randomized, open-label, parallel controlled clinical study. Cancer Commun., 42: 3-16.
- Mirhadi, E., F. Gheybi, N. Mahmoudi, M. Hemmati and F. Soleymanian *et al.*, 2022. Amino acid coordination complex mediates cisplatin entrapment within PEGylated liposome: An implication in colorectal cancer therapy. Int. J. Pharm., Vol. 623. 10.1016/j.ijpharm.2022.121946.
- 11. Dana, P., S. Bunthot, K. Suktham, S. Surassmo and T. Yata *et al.*, 2020. Active targeting liposome-PLGA composite for cisplatin delivery against cervical cancer. Colloids Surf. B: Biointerfaces, Vol. 196. 10.1016/j.colsurfb.2020.111270.
- 12. Zahednezhad, F., P. Zakeri-Milani, J.S. Mojarrad and H. Valizadeh, 2020. The latest advances of cisplatin liposomal formulations: Essentials for preparation and analysis. Expert Opin. Drug Delivery, 17: 523-541.
- Evers, M.J.W., S.I. van de Wakker, E.M. de Groot, O.G. de Jong and J.J.J. Gitz-François *et al.*, 2022. Functional siRNA delivery by extracellular vesicle-liposome hybrid nanoparticles. Adv. Healthcare Mater., Vol. 11. 10.1002/adhm.202101202.
- 14. Oh, H., B. Siano and S. Diamond, 2008. Neutrophil isolation protocol. J. Visual Exp., Vol. 17. 10.3791/745.
- 15. Zhang, H., Y. Liu, B. Yu and R. Lu, 2023. An optimized TRIzol-based method for isolating RNA from adipose tissue. BioTechniques, 74: 203-209.
- Elcik, D., A. Tuncay, E.F. Sener, S. Taheri and R. Tahtasakal *et al.*, 2021. Blood mRNA expression profiles of autophagy, apoptosis, and hypoxia markers on blood cardioplegia and custodiol cardioplegia groups. Braz. J. Cardiovasc. Surg., 36: 331-337.
- 17. Lee, J.H., S.H. Lee, E.H. Lee, J.Y. Cho and D.K. Song *et al.*, 2023. SCAP deficiency facilitates obesity and insulin resistance through shifting adipose tissue macrophage polarization. J. Adv. Res., 45: 1-13.
- 18. Huang, R.X. and P.K. Zhou, 2020. DNA damage response signaling pathways and targets for radiotherapy sensitization in cancer. Signal Transduction Targeted Ther., Vol. 5. 10.1038/s41392-020-0150-x.

- Węgierek-Ciuk, A., A. Lankoff, H. Lisowska, P. Kędzierawski, P. Akuwudike, L. Lundholm and A. Wojcik, 2021. Cisplatin reduces the frequencies of radiotherapy-induced micronuclei in peripheral blood lymphocytes of patients with gynaecological cancer: Possible implications for the risk of second malignant neoplasms. Cells, Vol. 10. 10.3390/cells10102709.
- Nagasawa, S., J. Takahashi, G. Suzuki, Y. Hideya and K. Yamada, 2021. Why concurrent CDDP and radiotherapy has synergistic antitumor effects: A review of *in vitro* experimental and clinical-based studies. Int. J. Mol. Sci., Vol. 22. 10.3390/ijms22063140.
- 21. Liu, C., L. Zhang, W. Zhu, R. Guo, H. Sun, X. Chen and N. Deng, 2020. Barriers and strategies of cationic liposomes for cancer gene therapy. Mol. Ther. Methods Clin. Dev., 18: 751-764.
- 22. Tsapras, P., S. Petridi, S. Chan, M. Geborys and A.C. Jacomin *et al.*, 2022. Selective autophagy controls innate immune response through a TAK1/TAB2/SH3PX1 axis. Cell Rep., Vol. 38. 10.1016/j.celrep.2021.110286.
- 23. Braun, H. and J. Staal, 2020. Stabilization of the TAK1 adaptor proteins TAB2 and TAB3 is critical for optimal NF- $\kappa$ B activation. FEBS J., 287: 3161-3164.
- 24. Morlino, S., A. Carbone, M. Ritelli, C. Fusco and V. Giambra *et al.*, 2019. *TAB2* c.1398dup variant leads to haploinsufficiency and impairs extracellular matrix homeostasis. Hum. Mutat., 40: 1886-1898.
- 25. Hori, A., O. Migita, R. Kawaguchi-Kawata, Y. Narumi-Kishimoto, F. Takada and K. Hata, 2021. A novel *TAB2* mutation detected in a putative case of frontometaphyseal dysplasia. Hum. Genome Var., Vol. 8. 10.1038/s41439-021-00166-6.
- Reineri, S., S. Agati, V. Miano, M. Sani and P. Berchialla et al., 2016. A novel functional domain of Tab2 involved in the interaction with estrogen receptor alpha in breast cancer cells. PLoS ONE, Vol. 11. 10.1371/journal.pone.0168639.
- Guan, S., L. Li, W.S. Chen, W.Y. Jiang and Y. Ding *et al.*, 2021.
   Circular RNA WHSC1 exerts oncogenic properties by regulating miR-7/TAB2 in lung cancer. J. Cell. Mol. Med., 25: 9784-9795.
- 28. Orecchioni, M., Y. Ghosheh, A.B. Pramod and K. Ley, 2019. Macrophage polarization: Different gene signatures in M1(LPS+) vs. classically and M2(LPS-) vs. alternatively activated macrophages. Front. Immunol., Vol. 10. 10.3389/fimmu.2019.01084.
- 29. Wang, L.X., S.X. Zhang, H.J. Wu, X.L. Rong and J. Guo, 2019. M2b macrophage polarization and its roles in diseases. J. Leukocyte Biol., 106: 345-358.
- Cutolo, M., R. Campitiello, E. Gotelli and S. Soldano, 2022. The role of M1/M2 macrophage polarization in rheumatoid arthritis synovitis. Front. Immunol., Vol. 13. 10.3389/fimmu.2022.867260.

- 31. Wang, Y., W. Smith, D. Hao, B. He and L. Kong, 2019. M1 and M2 macrophage polarization and potentially therapeutic naturally occurring compounds. Int. Immunopharmacol., 70: 459-466.
- 32. Kieler, M., M. Hofmann and G. Schabbauer, 2021. More than just protein building blocks: How amino acids and related metabolic pathways fuel macrophage polarization. FEBS J., 288: 3694-3714.
- 33. Cai, Y., J. Wen, S. Ma, Z. Mai and Q. Zhan *et al.*, 2021. Huang-Lian-Jie-Du decoction attenuates atherosclerosis and increases plaque stability in high-fat diet-induced ApoE<sup>-/-</sup> mice by inhibiting M1 macrophage polarization and promoting M2 macrophage polarization. Front. Physiol., Vol. 12. 10.3389/fphys.2021.666449.
- 34. Ganta, V.C., M. Choi, C.R. Farber and B.H. Annex, 2019. Antiangiogenic VEGF<sub>165</sub>b regulates macrophage polarization via S100A8/S100A9 in peripheral artery disease. Circulation, 139: 226-242.
- 35. Wang, D., X. Wang, M. Si, J. Yang and S. Sun *et al.*, 2020. Exosome-encapsulated miRNAs contribute to CXCL12/CXCR4-induced liver metastasis of colorectal cancer by enhancing M2 polarization of macrophages. Cancer Lett., 474: 36-52.
- Zhao, S., Y. Liu, L. He, Y. Li and K. Lin *et al.*, 2022. Gallbladder cancer cell-derived exosome-mediated transfer of leptin promotes cell invasion and migration by modulating STAT3-mediated M2 macrophage polarization. Anal. Cell. Pathol., Vol. 2022. 10.1155/2022/9994906.
- Li, H., F. Luo, X. Jiang, W. Zhang and T. Xiang *et al.*, 2022. CirclTGB6 promotes ovarian cancer cisplatin resistance by resetting tumor-associated macrophage polarization toward the M2 phenotype. J. Immunother. Cancer, Vol. 10. 10.1136/jitc-2021-004029.
- Miller, J.E., S.H. Ahn, R.M. Marks, S.P. Monsant, A.T. Fazleabas, M. Koti and C. Tayade, 2020. IL-17A modulates peritoneal macrophage recruitment and M2 polarization in endometriosis. Front. Immunol., Vol. 11. 10.3389/fimmu.2020.00108.
- 39. Lin, S.C., Y.C. Liao, P.M. Chen, Y.Y. Yang and Y.H. Wang *et al.*, 2022. Periostin promotes ovarian cancer metastasis by enhancing M2 macrophages and cancer-associated fibroblasts via integrin-mediated NF-κB and TGF-β2 signaling. J. Biomed. Sci., Vol. 29. 10.1186/s12929-022-00888-x.
- 40. Huang, X., C. Shen, Y. Zhang, Q. Li and K. Li *et al.*, 2019. Associations between *TAB2* gene polymorphisms and epithelial ovarian cancer in a Chinese population. Dis. Markers, Vol. 2019. 10.1155/2019/8012979.
- 41. Zhou, Y., Y. Liao, C. Zhang, J. Liu and W. Wang *et al.*, 2021. TAB2 promotes the stemness and biological functions of cervical squamous cell carcinoma cells. Stem Cells Int., Vol. 2021. 10.1155/2021/6550388.